World Academy of Science, Engineering and Technology
International Journal of Biotechnology and Bioengineering
Vol:4, No:8, 2010

Fe_3O_4 and Fe_3O_4@Au Nanoparticles: Synthesis and Functionalisation for Biomolecular Attachment

Hendriëtte van der Walt, Lesley Chown, Richard Harris, Ndabenhle Sosibo and Robert Tshikhudo

Open Science Index, Biotechnology and Bioengineering Vol:4, No:8, 2010 publications.waset.org/7836.pdf

***Abstract*—**The use of magnetic and magnetic/gold core/shell nanoparticles in biotechnology or medicine has shown good promise due to their hybrid nature which possesses superior magnetic and optical properties. Some of these potential applications include hyperthermia treatment, bio-separations, diagnostics, drug delivery and toxin removal. Synthesis refinement to control geometric and magnetic/optical properties, and finding functional surfactants for biomolecular attachment, are requirements to meet application specifics.

Various high-temperature preparative methods were used for the synthesis of iron oxide and gold-coated iron oxide nanoparticles. Different surface functionalities, such as 11-aminoundecanoic and 11-mercaptoundecanoic acid, were introduced on the surface of the particles to facilitate further attachment of biomolecular functionality and drug-like molecules. Nanoparticle thermal stability, composition, state of aggregation, size and morphology were investigated and the results from techniques such as Fourier Transform-Infra Red spectroscopy (FT-IR), Ultraviolet visible spectroscopy (UV-vis), Transmission Electron Microscopy (TEM) and thermal analysis are discussed.

***Keywords*—**Core/shell, Iron oxide, Gold coating, Nanoparticles.

I. Introduction

IRON oxide nanoparticles are widely studied materials as they occur naturally, are rapidly synthesised artificially, have attractive chemical and magnetic properties, and applications in *in vivo* magnetic imaging [1].

Iron oxide nanoparticles are inherently biocompatible [2] due to their general stability in air and their ability to be degraded or metabolised *in vivo*, making them excellent candidates for a large variety of applications [3]. Iron oxide nanoparticles have been extensively studied and applied in the biomedical field and, as a result, several commercial products have been made available for human diagnostics. Commercially available nanoparticles are typically coated by a biocompatible polymer, which improves the colloidal stability in physiological media and significantly reduces toxicity [4].

When surface modification involves a biomolecule like the FDA approved Poly (D,L-lactide-co-glycolide) (PLGA), surface coverage is critical, as is the ability of the molecule to retain its native conformation and binding profiles [5]. Polymer coating of magnetic nanoparticles have been well-documented as a method to improve the stability of the magnetic particles and to enhance their biological activity [6].

Of special interest are core/shell structured nanoparticles. These structures are not only ideal for studying proximity effects, but are also suitable for structure stabilisation, as the shell protects the core from oxidation and corrosion [7].

Gold coating of magnetic nanoparticles is a very attractive technique, as the magnetic nanoparticles can be both stabilised more effectively in corrosive biological conditions and easily functionalised through well developed Au-S chemistry. The coating also gives plasmodic properties to the magnetic nanoparticles, making them extremely useful for magnetic, optical and biological applications [6].

Our aim was to use the high-temperature solution phase reaction of $Fe(acac)_3$ to synthesise 11-aminoundecanoic acid (AUA) and 11-mercaptoundecanoic acid (MUA) stabilised Fe_3O_4 and Fe_3O_4@Au nanoparticles for possible further attachment of biomolecular functionalities and drug-like molecules. To elucidate the influence of the various biomolecularly modifiable stabilisers and the gold coating on the nature, stability and size of the iron oxide nanoparticles, FT-IR, TEM, UV-vis and thermal analysis methods were utilised.

II. Experimental Procedure

A. General

All chemicals were purchased from Sigma-Aldrich and used as received. The structures of the surfactants (AUA and MUA) used, are shown in Fig. 1 (a) and (b).

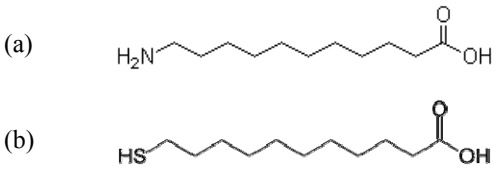

Fig. 1 Structures of surfactants: (a) 11-aminoundecanoic acid (AUA) and (b) 11-mercaptoundecanoic acid (MUA).

H. van der Walt, NIC, Advanced Materials Division, Mintek, Private Bag X3015, Randburg, 2125, South Africa (phone: +27 11 709 4757; fax: +27 11 709 4480; e-mail: hendriettep@mintek.co.za). All authors (L. Chown; R.A. Harris, N. Sosibo, R. Tshikhudo) Advanced Materials Division, Mintek, South Africa.

Open Science Index, Biotechnology and Bioengineering Vol:4, No:8, 2010 publications.waset.org/7836.pdf

B. Synthesis of Fe_3O_4 nanoparticles

The methods used to synthesise the nanoparticles are similar to that of other authors [8], [9]. Briefly: the surfactant AUA (0.604 g; 3 mmol) or MUA (0.656 g; 3 mmol) was added to $Fe(acac)_3$ (0.354 g; 1 mmol), 1,2-hexadecanediol (1.292 g; 5 mmol), oleyl amine (OLA) (988 µl; 3 mmol) and 10 ml phenyl ether in a round bottom flask under nitrogen. The mixture was heated to 200°C and refluxed for 2 hours. Ethanol was added to precipitate the particles after cooling of the solution. The particles were obtained and washed by centrifugation at 7000 r/min for 20 min and then finally redispersed in hexane.

C. Synthesis of Fe_3O_4@Au nanoparticles

Surfactant (AUA or MUA) stabilised Fe_3O_4 nanoparticles (1 ml) were added to a round-bottom flask under N_2 with 1, 2-hexadecanediol (0.302 g; 1.2 mmol), $Au(ac)_3$ (0.083 g; 0.22 mmol), surfactant AUA (30 mg; 0.15 mmol) or MUA (30 mg; 0.15 mmol), OLA (300 µl; 0.6 mmol) and 3 ml phenyl ether. The mixture was heated to 180-190°C and kept at this temperature for 1.5 hours. Particles were obtained as described previously for the Fe_3O_4 nanoparticles.

D. Nanoparticle characterisation

FT-IR spectra were measured with an Alpha Fourier Transform (FT)-Infrared spectrometer from Bruker®. The Attenuated Total Reflectance (ATR) attachment was used to collect 32 scans at a resolution of 2.

The UV-vis spectroscopy was conducted on a Perkin-Elmer, Lambda 35® UV-vis spectrometer, using diluted samples in hexane.

TEM imaging was performed on a Joel JEM 1010® Transmission Electron microscope. The sample (1 µl) was placed on a Formvar coated grid and dried before viewing.

Differential scanning calorimetry (DSC) and thermogravimetric analysis (TGA) were performed simultaneously using a Netzsch STA 429® with a Rhodium furnace. Dried samples were heated in N_2 to 100°C at a rate of 10°C.min^{-1} and held for 10 minutes to remove all surface-absorbed hexane. Thereafter, heating was continued at 10°C.min^{-1} to 1030°C. Results are expressed in µV.mg^{-1} (DSC) and in mass % (TG) as a function of temperature.

III. Results and Discussion

A. Particle Synthesis

As described in the experimental section monodisperse nanoparticles can be produced from the reduction of $Fe(acac)_3$ with various surfactants at high temperature, and then separated from the byproducts with ease. Although previous investigators [10] have reported that the key to uniform particles lies in the initial heating of the reaction mixture to 200°C for some time and then increasing the temperature to reflux, we illustrated that by increasing the temperature to 200°C and refluxing for 2 hours, uniform particles could be produced with less effort. The initial iron oxide nanoparticles appeared brown in solution, forming a black precipitate with the addition of ethanol. The solution turns bright red upon coating of the particles with gold.

B. FT-IR

The FT-IR spectra for the pure surfactants and the Fe_3O_4 stabilised nanoparticles are shown in Fig. 2.

Fig. 2 (a) and (b) show the pure surfactants (starting material) and surfactant stabilised Fe_3O_4 nanoparticles. Fig. 2 (c) compares the AUA and MUA stabilised Fe_3O_4.

The characteristic CH_2 and COOH peaks are noted for both the AUA and MUA surfactants, confirming the basic structure of the surfactant on the iron oxide nanoparticles. The NH_2 peaks were seen at 1439 cm^{-1} and 1421 cm^{-1} for the AUA stabilised nanoparticles. An overlap of the COO^- and NH_3^+ (1563 cm^{-1}) peaks was observed, indicating possible H bonding of the peripheral NH_2 groups. The weak SH peaks for the MUA stabilised Fe_3O_4 nanoparticles were not visible.

Fig. 2 also shows the transformation of the initial carboxylic acid (COOH – 1691 cm^{-1}) to a carboxyl ion (COO^- – 1582 cm^{-1} and 1706 cm^{-1}) when bonding occurred to stabilise the nanoparticles.

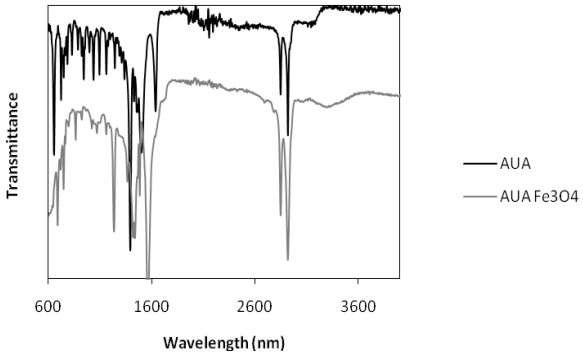

(a)

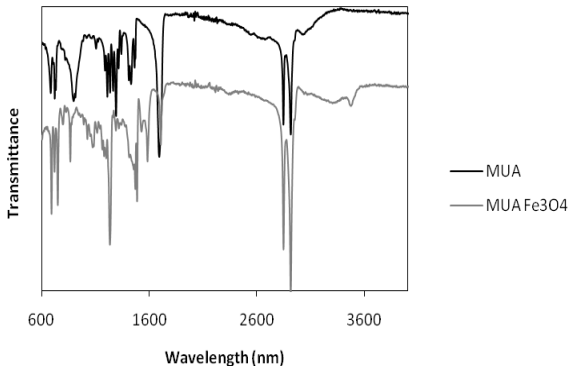

(b)

Open Science Index, Biotechnology and Bioengineering Vol:4, No:8, 2010 publications.waset.org/7836.pdf

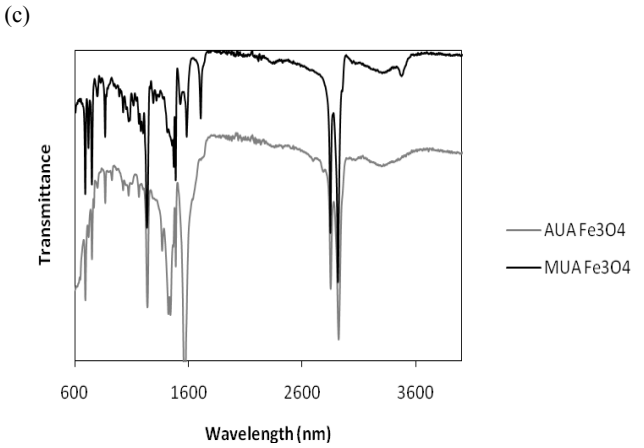

Fig. 2 FT-IR spectra of (a) AUA starting material and stabilised Fe_3O_4 nanoparticles; (b) MUA starting material and stabilised Fe_3O_4 nanoparticles; (c) Comparison of the AUA and MUA stabilised Fe_3O_4 nanoparticles.

C. UV absorbance

Fig. 3 showed that, as previously reported [11]-[12], there is no absorbance for the Fe_3O_4 nanoparticles, whereas absorbance was seen for the particles coated with gold. The absorbance of the 6 nm Au nanoparticles is included in Fig. 3 as reference and confirmation of the coating of the iron oxide nanoparticles. The absorbance value for the reference 6 nm Au nanoparticles was 518 nm, whereas the AUA stabilised Fe_3O_4@Au nanoparticles absorbed at 519 nm, indicating the similarity in size of the nanoparticles. The MUA stabilised Fe_3O_4@Au nanoparticles showed absorbance at 540 nm, indicating the large size difference between the AUA and MUA stabilised Fe_3O_4@Au nanoparticles.

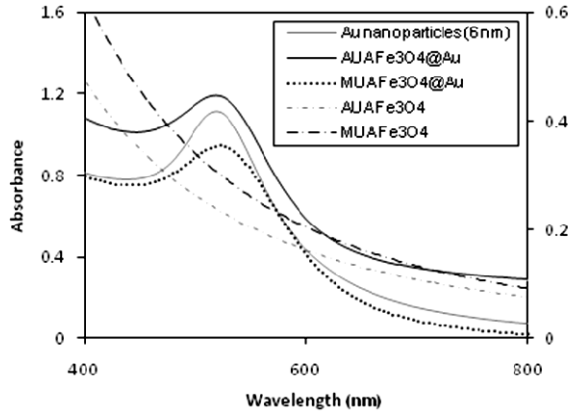

Fig. 3 UV-absorbance for the AUA and MUA stabilised Fe_3O_4 and Fe_3O_4@Au nanoparticles. The absorbance of 6 nm Au nanoparticles is included as reference and confirmation of the coating of the iron oxide nanoparticles.

D. TEM images

Structural images of the Fe_3O_4 and Fe_3O_4@Au nanoparticles are shown in Fig. 3.

As illustrated in Fig. 1, the structures for the AUA and MUA are identical except for the thiol and amine functional groups. It was predicted that the nanoparticles would be of similar size, but the TEM images in Fig. 4 (a) and (c) indicate a ± 1.25 nm variation in size (AUA 3.58 ± 0.75 nm; MUA 2.33 ± 0.69 nm) between the two Fe_3O_4 stabilised nanoparticle species. This may be due to H-bonding of the peripheral amine groups with additional absorbed AUA, which is supported by the FT-IR results and the large initial mass loss indicated by the TGA graph in Fig. 5 (a).

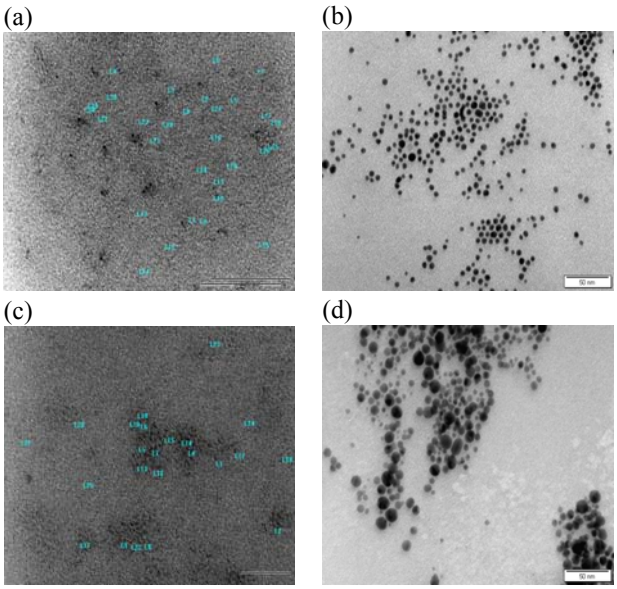

Fig. 4 TEM images of the AUA stabilised nanoparticles (a) Fe_3O_4 and (b) Fe_3O_4@Au and MUA stabilised nanoparticles (c) Fe_3O_4 and (d) Fe_3O_4@Au. Bars indicate 50 nm.

The AUA stabilised Fe_3O_4@Au nanoparticles showed little aggregation, with grouping of the particles indicating possible H-bonding. The MUA stabilised gold coated iron oxide nanoparticles showed greater aggregation and a wider size distribution (7.48 ± 2.32 nm) when compared to the AUA stabilized nanoparticles (4.97 ± 0.62 nm).

The large amount of aggregation could be due to either

1: the thiol as well as the carboxylic acid moieties bind to the surface of the Fe_3O_4@Au nanoparticles due to the affinity of gold for sulphur and the affinity of iron for oxygen or

2: the thiol binds to the Fe_3O_4@Au surface, while the peripheral carboxylic acids are bonded together by H-bond formation.

Previous reports [14] indicate the use of MUA as a cross-linking agent in the production of thin films. The cross-linking occurs between the thiols attached to the nanoparticles, and the carboxylic acids attach to each other due to H-bonding.

Open Science Index, Biotechnology and Bioengineering Vol:4, No:8, 2010 publications.waset.org/7836.pdf

Both potential reasons for the aggregation are being investigated.

E. Thermal Analysis

The DSC and TG results for the AUA and MUA stabilised nanoparticles are shown in Fig. 5. Fig. 5 (a) shows 3-stage and 2-stage mass changes for the MUA stabilised Fe_3O_4 and Fe_3O_4@Au nanoparticles respectively. The MUA Fe_3O_4@Au nanoparticles showed no change in mass above 650°C, while mass gain was seen for the Fe_3O_4 nanoparticles above 800°C. The DSC response, Fig. 5 (b) showed endothermic reactions associated with the onset of each mass loss step for the MUA stabilised Fe_3O_4 nanoparticles. Conversely, there are two broad exothermic peaks over the range of the 1st mass loss step for the MUA stabilised Fe_3O_4@Au nanoparticles, followed by an endothermic reaction at ~ 650°C.

Fig. 5 (c) shows 4-stage and 3-stage mass changes for the AUA stabilised Fe_3O_4 and Fe_3O_4@Au nanoparticles respectively. The DSC curve of the AUA stabilised Fe_3O_4 nanoparticles also showed endothermic peaks which correspond with the onset of the mass loss stages, but the reactions are smaller than the MUA stabilised nanoparticles. The AUA stabilised Fe_3O_4@Au DSC curve showed a small, broad exothermic peak over the ~ 200 - 600°C range, a small endothermic peak at 700°C and an exothermic peak at 820°C. The additional stages may be due to the initial removal of peripherally bonded AUA attached through H-bonding. The AUA Fe_3O_4@Au nanoparticles show no change in mass above 750°C, while mass gain is seen for the Fe_3O_4 nanoparticles above 950°C. This indicates that the gold coating may minimise oxidation of the Fe_3O_4 core at high temperature.

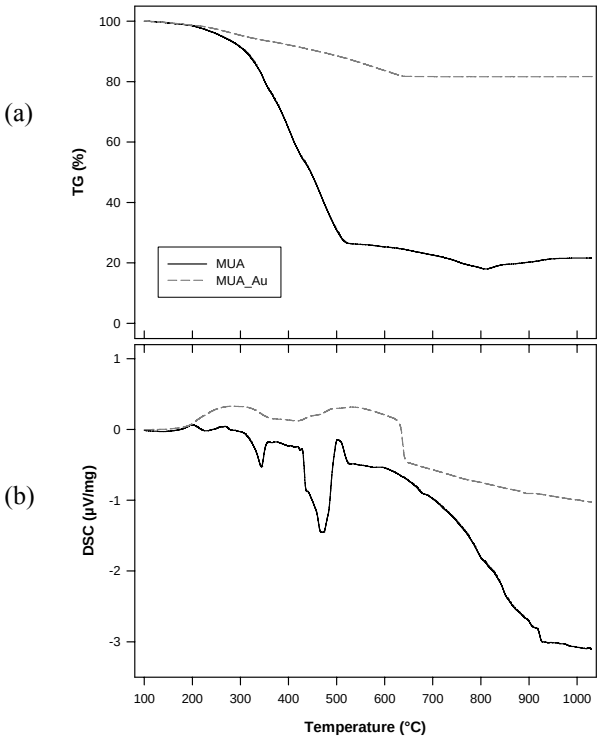

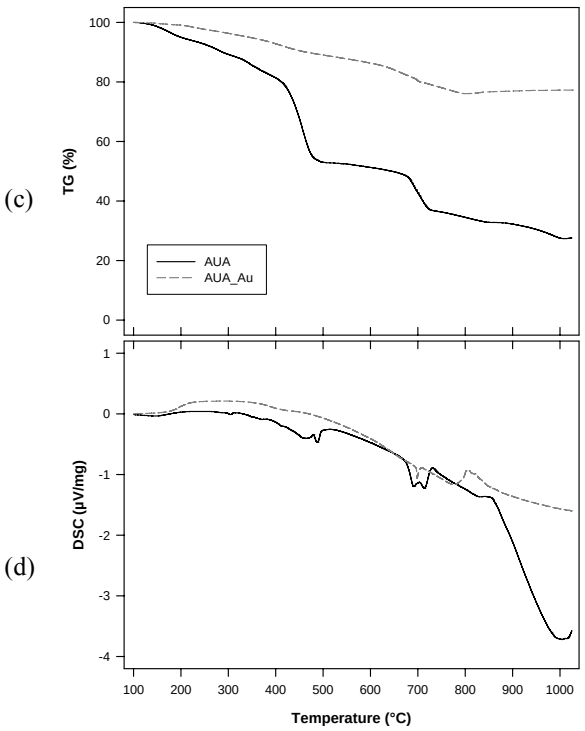

Fig. 5 Thermal analysis of the MUA stabilised Fe_3O_4 and Fe_3O_4@Au nanoparticles TGA (a) and DSC (b) and AUA stabilised Fe_3O_4 and Fe_3O_4@Au nanoparticles TGA (c) and DSC (d).

F. Further functionalisation

The initial plan was to stabilise Fe_3O_4 nanoparticles with various surfactants that would later be used to attach a variety of biomolecules and to coat these nanoparticles with gold. Amine and thiol moieties have been known to bind a variety of bio-functionalities and drug-like molecules. These functional groups would need to be on the periphery of the nanoparticle. This was observed for both the AUA and MUA stabilised Fe_3O_4 nanoparticles and the AUA stabilised Fe_3O_4@Au nanoparticles, making them good candidates for further functionalisation. The aggregation of the MUA stabilised Fe_3O_4@Au nanoparticles will, however, make it difficult to further utilise this functionality.

IV. Conclusion

Iron oxide and gold coated iron oxide nanoparticles were successfully synthesised. FT-IR confirmed the presence of the AUA and MUA surfactants on the nanoparticles, while the gold coating of the nanoparticles was confirmed by UV-vis spectrometry.

The sizes of the nanoparticles were determined by TEM. An increase in size of ± 1.25 nm, from the MUA Fe_3O_4 nanoparticles to the AUA Fe_3O_4 nanoparticles, indicates possible H-bonding on the periphery of the AUA stabilised

nanoparticles. Aggregation was seen for the MUA stabilised $Au@Fe_3O_4$ nanoparticles, whereas the AUA stabilised $Au@Fe_3O_4$ nanoparticles showed minimal aggregation with good size distribution.

Thermal analysis indicated that the $Fe_3O_4@Au$ nanoparticles showed greater stability, with ± 40% less mass loss than the nanoparticles without gold. The aggregation of the MUA stabilised $Au@Fe_3O_4$ nanoparticles prevents the use of it for further functionalisation.

ACKNOWLEDGMENT

We would like to thank The University of KwaZulu-Natal for the TEM analysis. We would also like to thank Mintek and AuTEK (Gold Fields) for permission to publish the paper and for financial support.

REFERENCES

[1] A. Cabot, V. F. Puntes, E. Shevchenko, Y. Yin, L. Balcells, M. A. Marcus, S. M. Hughes, and A. P. Alivisatos, "Vacancy coalescence during oxidation of iron nanoparticles", *J. Am. Chem. Soc.*, vol. 129, no. 34, pp. 10358-10360, 2007.

[2] I. Koh, X. Wang, B. Varughese, L. Isaacs, S.H. Erhman, and D.S. English, "Magnetic iron oxide nanoparticles for biorecognition: evaluation of surface coverage and activity", *J. Phys. Chem. B*, vol. 110, no. 4, pp. 1553-1158, 2006.

[3] L.M. Bronstein, X. Huang, J. Retrum, A. Schmucker, M. Pink., B.D. Stein, and B. Dragnea, "Influence of iron oleate complex structure on iron oxide nanoparticles formation", *Chem. Mater.*, vol. 19, no. 15, pp. 3624-3632, 2007.

[4] J-F. Lutz, S. Stiller, A. Hoth, L. Kaufer, U. Pison, and R. Cartier, "One-pot synthesis of PEGylated ultrasmall iron-oxide nanoparticles and their in vitro evaluation as magnetic resonance imaging contrast agents", *Biomacromolecules*, vol. 7, no. 11, pp. 3132-3138, 2006.

[5] S-J. Lee, J-R. Jeong, S-C. Shin, J-C. Kim, Y-H. Chang, K-H. Lee, and J-D. Kim, "Magnetic enhancement of iron oxide nanoparticles encapsulated with poly(D,L-latide-co-glycolide)", *Colloids and Surfaces A: Physicochem. Eng. Aspects*, vol. 255, pp. 19-25, 2005.

[6] Z. Xu, Y. Hou, and S. Sun, "Magnetic core/shell Fe_3O_4/Au and Fe_3O_4/Au/Ag nanoparticles with tunable plasmodic properties", *J. Am. Chem. Soc*., vol. 129, no. 28, pp. 8698-8699, 2007.

[7] S-J. Cho, J-C. Idrobo, J. Olamit, K. Liu, N.D. Browning, and S.M. Kauzlarich, "Growth mechanisms and oxidation resistance of gold-coated iron nanoparticles", *Chem. Mater*. vol. 17, no. 12, pp. 3181-3186, 2005.

[8] P. Gangopadhyay, S. Gallet, E. Franz, A. Persoons, and T. Verbiest (). "Novel superparamagentic core(shell) nanoparticles for magnetic targeted drug delivery and hyperthermia treatment", *IEEE Transactions on Magnetics* vol. 41, no. 10, pp. 4194-4196, 2005.

[9] W. Wang, L. Luo, Q. Fan, M. Suzuki, I.S. Suzuki, M.H. Engelhard, Y. Lin, N. Kim, J.Q. Wang, and C-J Zhong, "Monodispersed core-shell FeO@Au nanoparticles", *J. Phys. Chem. B*, vol. 46, no. 109, pp. 21593-21601, 2005.

[10] S. Sun, and H. Zeng, "Size-controlled synthesis of magnetic nanoparticles", *J. Am. Chem. Soc*., vol. 124, no. 28, pp. 8204-8205, 2002.

[11] J-H. Huang, H.J. Parab, R-S. Liu, T-C. Lai, M. Hsiao, C-H. Chen, H-S. Sheu, J-M. Chen, D-P. Tsai, and Y-K. Hwu, "Investigation of the growth mechanism of iron oxide nanoparticles via a seed-mediated method and its cytotoxicity studies", *J. Phys. Chem. C,* vol. 112, no. 40, pp. 15684-15690, 2008.

[12] S. Sun, H. Zeng, D.B. Robinson., S. Raoux, P.M. Rice, S.X. Wang, and G. Li, "Monodisperse MFeO (M = Fe, Co, Mn) nanoparticles", *J. Am. Chem. Soc*., vol. 126, no. 1, pp. 273-279, 2004.

[13] H.L. Liu, C.H. Sonn, J.H. Wu, K-M. Lee, and Y.K. Kim, "Synthesis of streptavidin-FITC-conjugated core-shell Fe_3O_4-Au nanocrystals and their application for the purification of $CD4^+$ lymphocytes", *Biomaterials*, vol. 29, pp. 4003-4011, 2008.

[14] L. Wang, J. Luo, Q. Fan, M. Suzuki, I.S. Suzuki, M.H. Engelhard, Y. Lin, N. Kim, J.Q. Wang, C-J. Zhong, "Monodispersed core-shell Fe_3O_4@Au nanoparticles", *J. Phys. Chem. B,* vol. 109, no. 46, pp. 21593-21601, 2005.

Open Science Index, Biotechnology and Bioengineering Vol:4, No:8, 2010 publications.waset.org/7836.pdf